MOLECULAR PHYSICS, 1986, VOL. 58, NO. 6, 1067–1085

Highly rotationally excited states of floppy molecules: H_2D^+ with $J \leqslant 20$.

by JONATHAN TENNYSON
Department of Physics and Astronomy, University College London, Gower Street, London WC1E 6BT, England

and BRIAN T. SUTCLIFFE
Chemistry Department, University of York, Heslington, York YO1 5DD, England

(*Received 12 March 1986; accepted 28 March 1986*)

A partitioning of the generalized triatomic hamiltonian of the preceding paper is developed which allows the calculation of highly-excited rotational states, without approximation, in a two-step variational procedure. Iterative diagonalization techniques are found to be particularly useful for the second variational step. The rotationally-excited states of H_2D^+ are studied with $J \leqslant 20$, well into the region where the ground and excited state manifolds overlap. Comparison of results for two different *ab initio* potentials and convergence considerations suggest that pure rotational transition frequencies obtained from our results should be accurate to about 1 cm^{-1} for $J \sim 15$.

1. INTRODUCTION

The *a priori* computation of ro-vibrational spectra of small molecules, mainly triatomic, has made significant progress over the last decade, but has been largely confined to low values of the total angular momentum quantum number, J. The reasons for this are twofold, firstly most experimental information has come from transitions between moderately low values of J (although often much higher than has been calculated) and secondly, and more crucially, the size of a fully coupled ro-vibrational calculation increases rapidly with J and soon become intractable. Fully coupled calculations have generally been limited to $J \leqslant 4$ [1–5].

This lack of work on highly excited rotational states does not mean that these states are without interest. They are, for example, crucial for testing and refining our ideas on model hamiltonians [6] based as they are on perturbation coupling schemes which may cease to be valid in the high J limit.

In such a coupling scheme, it is usual to regard the rotational levels of a system as a sub-manifold of a particular vibrational state. Although coupling between rotational levels of different vibrational manifolds through Coriolis interactions is well-known, it is generally regarded as a (small) perturbation. Many theoretical analyses of large J states have ignored this interaction (e.g. [7]). We will call the region where this approximation is valid the low J regime, while realizing that for heavy molecules this regime may include J values of several

hundred. A semi-quantitative definition of the range of the regime is given by considering the ratio of the rotational and vibrational splittings, R_J, which can be approximated by

$$R_J \simeq [A - (B + C)/2]J^2/\omega, \tag{1}$$

where A, B and C are the usual rotational constants and ω the lowest vibrational fundamental for the molecule. In the low J regime R_J is very much less than unity. However, as J increases so does the width of the rotational manifold that is the difference between levels with $\tau = -J$ and $\tau = +J$ for an asymmetric top, or $K = 0$ and $K = J$ for a symmetric top. For higher J, R_J will approach unity and at this point rotational sublevels of the ground vibrational state will begin to overlap the rotational manifold of the lowest vibrationally-excited state. This we call the intermediate J region.

For high enough J, the situation will arise where the rotational splittings are much larger than the spacing between vibrational levels, $R_J \gg 1$. In the extreme, this would result in the re-ordering of the quantum numbers (or perturbative coupling scheme) so that levels with low K, in the symmetric top case, will be preferred and the vibrational parentage of a state will become the small perturbation. This recoupling for large values of the total angular momentum is well-known in nuclei [8] where the study of 'high spin states' is an area of considerable activity. To our knowledge, such recoupling has yet to be observed in molecular systems, but, as we demonstrate, is not outside the scope of current experiments.

In this paper we propose a tractable procedure for the *ab initio* calculation of highly excited rotational states with full ro-vibrational coupling. This procedure, based on the use of a secondary variational step in the calculation, is similar to the method used recently by Chen *et al.* [9] for calculating the low-lying states of H_2O with $J \leqslant 10$. However, it differs in one respect which we expect to be important for the accurate calculation of the highly-excited states considered here.

Light systems, with large rotational constants, will tend to display the high J effects at lower values of the total angular momentum than heavier systems. H_3^+, the lightest (and electronically simplest) polyatomic system thus makes a suitable starting point for such a study. The low-lying ro-vibrational states of H_3^+ and its isotopomers have been the subject of much recent study, both experimentally and theoretically, and a fair measure of understanding has been achieved for these states [4]. In particular, H_2D^+ is known to be a highly-asymmetric top, $\kappa \simeq -0{\cdot}07$, whose vibrational levels show strong Coriolis coupling due to the splitting of levels degenerate in H_3^+ [2]. However, all the calculations on H_2D^+ have concentrated on states with low $J(\leqslant 4)$, and the published experiments have been confined to $J \leqslant 7$ [2, 10–13]. There is, however, evidence to show that for H_2D^+ transitions involving large values of J, in the range 20–30, cannot be interpreted using the rotational constants determined from the study of low J states [14]. For these high J levels one might anticipate an R_J significantly greater than one.

In this work we consider the ro-vibrational states of H_2D^+ with $J \leqslant 20$ in a first attempt for a realistic system to analyse theoretically the breakdown of ro-vibrational structure. The accurate knowledge of the electronic potential for H_3^+ gives us some confidence in the reliability of our calculations, although we also test this by comparing results obtained using different potentials.

2. Theory

In the previous paper [15], hereafter referred to as I, we developed a generalized ro-vibrational hamiltonian for triatomics in any internal co-ordinate system which consists of two lengths and an angle. This hamiltonian was written

$$H = K_V^{(1)} + K_V^{(2)} + K_{VR}^{(1)} + K_{VR}^{(2)} + V, \tag{2}$$

where the K_V terms are pure vibrational kinetic energy operators, and the K_{VR}s are vibration–rotation kinetic energy operators, which are zero for $J = 0$. The terms superscripted 2 are those introduced by the generalization of the co-ordinates from atom–diatom scattering co-ordinates. V is the electronic potential.

In this work we first diagonalize a hamiltonian for which k, the projection of J onto the body-fixed z axis, is a good quantum number, and then we tackle the full problem. In this way, we aim to reduce the size of the full problem that need be considered. A solution of the hamiltonian

$$H_{J,k} = K_V^{(1)} + K_V^{(2)} + \delta_{kk'} K_{VR}^{(1)} + V, \tag{3}$$

with eigenvalue $\varepsilon_i^{J,k}$ can be written

$$\phi_i^{J,k} = \sum_{j,m,n} c_{j,m,n}^{J,k,i} H_m(r_1) H'_n(r_2) \Theta_{jk}(\theta) D^J_{Mk}(\alpha, \beta, \gamma) \tag{4}$$

in terms of the basis functions developed in I. We note that the eigenvalues are independent of the sign of k.

These eigenvectors can then be used as a basis set for the full hamiltonian (2). The matrix elements for this second step are

$$\begin{aligned}\langle k', i' | H | k, i\rangle = {} & \delta_{k'k}\delta_{i'i}\varepsilon_i^{J,k} + f(k, k')\delta_{k',k\pm1} C^{\pm}_{J,k} \sum_{jmn}\sum_{j'm'n'} c_{j,m,n}^{J,k,i} c_{j'm'n'}^{J,k',i'} \\ & \times \Bigg\{ \delta_{j'j}\delta_{n'n} C^{\pm}_{jk} \langle m' | \frac{1}{2\mu_1 r_1^2} | m\rangle \\ & + \delta_{j',j+1} \frac{a_{j,\pm k}}{2\mu_{12}} \langle m' | \frac{1}{r_1} | m\rangle \left[(j+1)\langle n' | \frac{1}{r_2} | n\rangle + \langle n' | \frac{d}{dr_2} | n\rangle \right] \\ & + \delta_{j',j-1} \frac{b_{j,\pm k}}{2\mu_{12}} \langle m' | \frac{1}{r_1} | m\rangle \left[j\langle n' | \frac{1}{r_2} | n\rangle - \langle n' | \frac{d}{dr_2} | n\rangle \right] \Bigg\},\end{aligned} \tag{5}$$

for z embedded along $\mathbf{r}_1$ (and the same with $r_2 \leftrightarrow r_1$, $\mu_1 \leftrightarrow \mu_2$ and $m \leftrightarrow n$ interchanged for z embedded along $\mathbf{r}_2$). The factors $a_{j,k}$ and $b_{j,k}$ are defined in I and

$$\left.\begin{aligned} f(k, k') &= 1, && k, k' > 0 \quad \text{or} \quad k' = k = 0, \\ &= 2^{1/2}, && k = 0, \quad k' = 1 \quad \text{or} \quad k = 1, \quad k' = 0, \end{aligned}\right\} \tag{6}$$

is included to account for the symmetrization of the basis with respect to the total parity:

$$\left.\begin{aligned} |k, i\rangle &= \frac{1}{\sqrt{2}} (\phi_i^{J,k} + (-1)^p \phi_i^{J,-k}), && p = 0, 1; \quad k > 0, \\ &= \phi_i^{J,k}, && p = 0, \quad k = 0, \end{aligned}\right\} \tag{7}$$

where, by convention, $p = 0$ for the e block and $p = 1$ for the f block. The total parity is given by $(-1)^{J+p}$. We note that no matrix elements appear in (5) for which $|k - k'|$ is greater than one.

Clearly, if all the solutions of hamiltonian (3) are used to diagonalize the full hamiltonian (2), then the results should be identical to those obtained by letting the full hamiltonian act on the untransformed basis functions. However, it is possible that not all the solutions of $H_{J,k}$ are needed if one is only interested in a few, low-lying levels of H. Furthermore, as the secular equation method is variational, convergence from above can, in general, be demonstrated.

The secondary variational procedure outlined here has one important difference to the method used for their calculations on water by Chen *et al.* [9]. The hamiltonian of their first variational step, which was actually expressed in normal displacement co-ordinates, omitted the term equivalent to the diagonal part of $K_{VR}^{(1)}$ which we include. This has the advantage that their first variational step is independent of J and hence the $J = 0$ vibrational wavefunctions (for $J = 0$, $H_{J,k}$ is the exact hamiltonian) can be used as the basis for all J states. However, these basis functions will not allow for the shifts in geometry caused by the centrifugal terms in the potential, which, as we will show, are large in the high J region. Chen *et al.*'s calculations, although considering J up to 10, were entirely confined to the low J, $R_J \ll 1$ region. A similar procedure has also recently been used by Spirko *et al.* on H_3^+ and H_2D^+, but only for $J \leqslant 4$ [5].

The theory given here is for the generalized co-ordinates of I; in this work we consider H_2D^+ in scattering co-ordinates. That is a system with r as the H_2 bondlength, R joining the H_2 midpoint with D and θ the angle between **r** and **R**. This co-ordinate system is the best alternative within this formalism for the H_3^+ isotopomers as shown by the calculations on D_2H^+ in I. Furthermore, we will embed the z axis along R, making $r_1 = R$ and $r_2 = r$ in the above analysis. Test calculations and previous experience [1–3] having shown this to be the best embedding for this system.

3. Practical considerations

If the procedure outlined above is to work three problems must be borne in mind: convergence of the first variational step, convergence of the second variational step and the computational tractability of the procedure, especially for large values of J. The first variational step is very similar to the pure, $J = 0$, vibrational problem—the centrifugal distortion terms can be considered as extra isotropic terms in the potential. There is considerable experience in converging these vibrational problems [16] and the only added problem is that of developing a basis appropriate for a range of k values.

Table 1 demonstrates the convergence of the second variational step for the low-lying states of H_2D^+ with $J = 4$. The symmetry block is that with even total parity and even (para) with respect to interchange of the two H atoms. For comparison, the 'exact' variational results are also given, that is the result obtained by directly diagonalizing the full ro-vibrational problem. These results are the same as those obtained by including all the eigenfunctions of the first step in the basis used for the second step, which demonstrates the numerical stability of our procedure. However, it is clear from table 1 that, at least for low J, only a fraction of these functions are needed to converge the second variational step.

The matrices obtained in the second variational step have a structure which means that they become increasingly sparse with J. The only non-zero elements are the purely diagonal ones in the diagonal block where $k = k'$, and all those in

Table 1. Convergence of $J = 4^e$ rotational levels with vibrational basis (N). Energies are relative to $E_0 = -32962{\cdot}259\,\mathrm{cm}^{-1}$. The 'exact' calculation is that of table 8 of [1]. The 'No Coriolis' results are for z embedded along **R**.

	Wavenumbers/cm^{-1}							
	$v = 0$			$v_2 = 1$ and $v_3 = 1$ [2]				
	$k = 0$	$k = 2$	$k = 4$	$k = 0$	$k = 2$	$k = 1$	$k = 4$	$k = 3$
No Coriolis	558·829	624·859	809·570	2766·643	2824·804	2837·643	2981·974	3022·108
$N = 20$	402·628	580·727	778·153	2522·524	2752·245	2767·909	2946·105	2984·913
40	402·336	580·701	778·137	2519·251	2751·725	2767·593	2945·973	2984·745
60	402·311	580·699	778·136	2518·983	2751·688	2767·572	2945·963	2984·738
80	402·310	580·699	778·136	2518·981	2751·688	2767·571	2945·963	2984·738
'Exact' $N = 200$	402·310	580·699	778·136	2518·98	2751·69	2767·57	2945·96	2984·74

the leading off-diagonal blocks with $k = k' \pm 1$. If N solutions of the first variational step are used, the secular matrix has only $(J - p)N(N + 1) - N^2$ unique elements out of a total of $(J - p + 1)^2N^2$.

Table 2 compares the performance of 3 diagonalizers on a problem with $J = 10^e$ and $N = 82$—the largest problem for which the entire matrix could be handled in core. The most notable feature of table 2 is the wide variation in memory required by the three diagonalizers. The first diagonalizer, which retained the entire matrix in core, assumed only that it was symmetric. The second diagonalizer treated the matrix as banded and symmetric, and thus required approximately twice the minimum amount of storage as the band width is $2N$. The third diagonalizer uses an iterative algorithm designed for sparse matrices. Because of the known structure of the matrix it was possible not only to retain the minimum number of matrix elements, but also to use this structure to simplify the vector matrix multiplication required on each iteration. Care was taken to ensure that this multiplication was vectorized. The iterations were started from unit vectors determined by the ordering of the diagonal elements and converged to a tolerance which gave the eigenvalues accurately to $0{\cdot}01\ \mathrm{cm}^{-1}$. All the diagonalizers agreed to this accuracy. Both the full and banded diagonalizers were taken from a package that has been vectorized [17].

As can be seen from table 2, the banded matrix diagonalizer was the slowest. The iterative procedure was found to be the most efficient, both in core and CPU time.

For $J = 10$, the time taken for the second diagonalization is modest compared to solving eleven 504 dimensional base problems, with k equals 0 to 10 inclusive, and similar to that taken to construct the final secular matrix. However, the time taken for both these steps increases only linearly with J. Our bigger calculations, the largest of which was for a matrix of dimension 3780, depended strongly on the time taken for the final diagonalization.

Using the iterative diagonalization procedure and an eigenvalue tolerance of $0{\cdot}01\ \mathrm{cm}^{-1}$, we next considered the convergence characteristics of the two variational steps for higher values of J. Test calculations showed that the basis set optimized by us previously for low J calculations [1], and used in table 1, gave a poor representation of states with large k, particularly $k > 10$. For these states, the centrifugal terms are large and it was found necessary to increase the flex-

Table 2. Comparison of computational requirements for three diagonalization procedures for the 902 dimensional secular problem given by $J = 10^e$ and $N = 82$. 17 eigenvalues and eigenvectors were obtained for the same secular matrix which took 8·2 s to construct. Requirements for the base problems, the first variational step, are shown for comparison.

Diagonalization method	Storage (words)	Time (Cray-1/s)
Full matrix [17]	849,424	21·58
Banded matrix [18]	183,748	59·26
Sparse matrix [19]	103,973	11·75†
Base Problem [20]		
200 × 200	76,668	11 × 2·10
504 × 504	285,979	11 × 15·85

† Tolerance 10^{-3}, giving 8 figure ($0.01\ \mathrm{cm}^{-1}$) accuracy in the eigenvalues.

Table 3. Convergence of 4 typical calculations which neglect Coriolis interactions with increasing basis set size. Energies are relative to the $D^+ + H_2$ dissociation limit in cm^{-1}.

			Wavenumbers/cm^{-1}			
m^{max}†	n^{max}‡	j^{max}§	$J = 0$, $k = 0$ $j^{max} = 14$	$J = 20$, $k = 0$ $j^{max} = 14$	$J = 20$, $k = 20$ $j^{max} = 30$	$J = 30$, $k = 30$ $j^{max} = 40$
4	4	j^{max}	−32953·095	−23123·595	−19056·013	−8263·127
4	4	$j^{max} + 4$	−32953·097	−23123·595	−19056·013	−8263·127
4	6	j^{max}	−32953·218	−23123·910	−19056·108	−8264·003
4	8	j^{max}	−32953·222	−23123·933	−19056·109	−8264·004
6	4	j^{max}	−32961·327	−23140·856	−19056·908	−8288·554
8	4	j^{max}	−32962·111	−23142·538	−19056·932	−8289·119
10	4	j^{max}	−32962·178	−23142·706	−19056·934	−8289·376
Optimized						
8	6	j^{max}	−32962·240	−23142·888	−19057·021	−8291·499

† Morse-like functions $H_m(r)$ with $m = 0$ to m^{max} and $r_e = 2{\cdot}2\,a_0$, $\omega_e = 0{\cdot}007E_h$ and $D_e = 0{\cdot}07E_h$ [20]

‡ Morse-like functions $H'_n(r)$ $n = 0$ to n^{max} and $R_e = 1{\cdot}55\,a_0$, $\omega_e = 0{\cdot}008\,E_h$ and $D_e = 0{\cdot}215\,E_h$ [20]

§ Associate Legendre polynomials $\Theta_{jk}(\theta)$ with $j = k$ to j^{max}.

ibility of the radial basis functions to allow for rotational distortions. It was also found necessary to increase j^{max}, the order of the highest Legendre function in the basis, although the condition that $j \geqslant k$ means that this did not lead to an increase in the size of the angular basis. Table 3 presents results for our re-optimized basis and demonstrates convergence for a selection of vibrational calculations.

Using the optimized basis for the first variational step given in table 3, tables 4, 5 and 6 show the convergence of calculations with $J = 10$, 15 and 20 with increasing basis. All these calculations are e parity with j even as this symmetry gives the densest spectrum and hence the slowest convergence properties. The levels analysed correspond to those that might be thought of as stemming from the ground and first two vibrationally-excited states ($v_2 = 1$ and $v_3 = 1$), determined simply on energy ordering. It can be seen that in all cases the results are converging, although this convergence is slower as J increases. The convergence

Table 4. Convergence of some levels with $J = 10^e$ (j even) with increasing vibrational basis, N. Energies, in cm^{-1}, are all relative to $E_0 = -32962{\cdot}24$. k, the projection of J along **R**, values are taken from the No-Coriolis calculations.

	Wavenumbers/cm^{-1}					
Level number	1	4	7	10	13	16
$k =$	0	6	1	2	6	10
No Coriolis	2928·04	3575·06	4993·32	5255·81	5793·80	6411·49
$N = 40$	1982·24	3182·15	4192·20	4914·70	5274·42	5705·53
80	1977·14	3181·48	4191·37	4908·68	5270·12	5702·15
120	1976·66	3181·40	4191·35	4907·86	5269·14	5701·30
140	1976·53	3181·39	4191·34	4907·26	5269·07	5701·25
160	1976·53	3181·39	4191·34	4907·19	5269·02	5701·21
180	1976·52	3181·39	4191·34	4907·11	5268·98	5701·17

Table 5. Convergence of some $J = 15^e$ (j even) levels with increasing N. See legend to table 4 for further explanation.

	Wavenumbers/cm^{-1}					
Level number	1	4	7	10	13	16
$k =$	0	6	10	2	4	0
No Coriolis	6018·88	6799·41	7861·42	8337·03	8614·36	9072·26
$N =$ 40	4154·92	6047·04	6609·22	7173·86	7698·90	8099·87
80	4128·18	5932·57	6554·57	7103·85	7660·20	7979·43
120	4126·30	5922·71	6549·38	7092·55	7650·89	7973·82
160	4123·27	5904·88	6539·20	7084·78	7647·86	7969·43
180	4123·13	5904·20	6538·34	7083·89	7647·35	7969·02
200	4123·04	5903·39	6537·62	7083·23	7646·19	7968·62

Table 6. Convergence of some $J = 20^e$ (j even) levels with increasing N. See legend to table 4 for further explanation.

	Wavenumbers/cm^{-1}					
Level number	1	2	4	6	8	10
$k =$	0	2	6	1	10	12
No Coriolis	9819·4	9927·2	10729·4	11351·3	12049·6	12762·1
$N =$ 40	7039·5	8083·5	8896·3	9503·9	10012·6	10189·3
80	6981·2	8032·4	8825·9	9445·8	9886·0	10132·8
120	6968·4	8024·4	8819·8	9439·0	9881·5	10127·1
160	6958·5	8012·7	8809·3	9429·5	9874·0	
180	6957·2	8011·8	8808·6	9428·6	9870·9	10119·8

with the re-optimized basis is also slower than that observed by us in test calculations using the smaller basis of table 1. This is because the spectrum of vibrational levels given by the larger re-optimized basis is denser. A feature shown by analysing convergence rates is that the lower levels do not necessarily converge quicker—for example, compare the lowest level in table 4 with level numbers 4 and 7. This is because the Coriolis interactions for states with low k are considerably stronger than those with high k, due to the angular coefficient $C^{\pm}_{Jk}$, see I. Another obvious feature is that neglecting the Coriolis interactions is a poor approximation for H_2D^+. The tables show that for $N = 180$, the $J = 10^e$ levels are converged to about 0·1 cm^{-1}, $J = 15^e$ to about 1 cm^{-1} and the $J = 20^e$ levels to about 5 cm^{-1}. Although we would like to consider Js higher than 20, this must await a time when this level of convergence can be improved upon.

4. Results

Calculations were performed using the optimized basis of table 3 for the first variational step. The angular basis set parameter j^{max} was incremented from 14 for $k = 0$ to 34 for $k = 20$. Thus for each J it was necessary to diagonalize $J + 1$ secular problems of dimension 504 as calculations with $p = 0$ and $p = 1$ (e and f) use the same basis. For the second variational step $N = 180$ was used for all J. This was done for consistency, even though for lower J values it gave convergence considerably better than required. For each J value and symmetry

block, the diagonalization was converged to 0·01 cm^{-1} for sufficient levels to cover approximately, the rotational manifold of the lowest three vibrational states.

Throughout this work the potential of Schinke, Dupuis and Lester [21] has been used, for previous work had shown it to provide a very good representation of the low-lying rotational states, reproducing experiment to about 0·1 per cent [12, 22]. However our previous calculations have shown that the BVDH potential fitted by Martire and Burton [23] to the *ab initio* data of Burton *et al.* [24] gives better results for the vibrational excitation energies than does the SDL potential. It was therefore thought appropriate to compare the effectiveness of these two potentials in high J calculations. The results of such a comparison, for $J = 16^e$, are shown in table 7. Tables 8 to 11 give the calculated levels for H_2D^+ with J up to 20 for the four symmetry blocks using the SDL potential and table 12 compares our labelling of the symmetry blocks with other labelling schemes.

In all the tables 7 to 11, the frequencies of the levels are given relative to the $J = 0$ vibrational ground state of H_2D^+. From these and the appropriate selection rules ($\Delta J = 0, \pm 1$; $\Delta K_a = 0, 2, \ldots$; $\Delta K_c = 1, 3, \ldots$) a list of predicted transition frequencies has been constructed, copies of which can be obtained from the authors. It was however not possible to label all states with values of (K_a, K_c). This is because of the increasing overlap between rotational manifolds of different vibrational states. This behaviour is also reflected in the k values of the No Coriolis results presented in tables 4 to 6.

Table 7. Comparison of the $J = 16^e$ rotational levels for two *ab initio* potentials.

State number	Wavenumbers/cm^{-1}					
	j even			j odd		
	SDL	BVDH	Δ	SDL	BVDH	Δ
1	4637·44	4631·65	5·79	4635·27	4629·55	5·72
2	5548·71	5543·06	5·75	5548·69	5543·05	5·74
3	6225·05	6221·07	3·98	6224·96	6221·01	3·95
4	6396·56	6407·87	−11·31	6384·25	6395·78	−11·53
5	6708·13	6705·12	3·01	6724·40	6722·34	2·06
6	6974·50	6973·50	1·00	7045·34	7058·78	−13·44
7	7047·51	7060·82	−13·31	7155·42	7155·16	0·26
8	7410·17	7411·04	−0·79	7420·40	7424·55	−4·15
9	7424·76	7427·91	−3·15	7597·19	7590·44	6·75
10	7600·36	7593·25	7·11	7708·41	7707·83	0·58
11	7881·93	7898·16	−16·77	7882·19	7898·39	−16·20
12	8031·74	8030·82	0·92	8217·33	8218·21	−0·88
13	8217·49	8218·32	−0·83	8302·88	8320·29	−17·41
14	8332·45	8349·57	−17·12	8373·36	8372·65	0·71
15	8434·39	8452·08	−17·69	8436·18	8453·43	−17·25
16	8538·20	8533·10	5·10	8538·54	8533·70	4·84
17	8637·12	8668·04	−30·92	8626·69	8657·11	−30·42
18	8723·24	8723·49	−0·25	8787·67	8799·54	−11·87
19	8812·47	8813·61	−1·14	8861·19	8874·49	−13·30
20	8867·55	8891·82	−14·27	9059·71	9069·81	−10·10
21	9147·64	9142·84	4·80	9067·90	9081·49	−13·59
22	9171·11	9176·04	−4·93	9155·02	9160·86	−5·84
23	9196·02	9196·27	−0·25	9210·06	9230·00	−19·94
24	9335·83	9356·46	−20·63	9323·17	9325·22	−2·05

Table 8. H_2D^+ rotational levels with j even and e ($p = 0$) total parity relative to the $J = 0$ ground state at $-32962{\cdot}24\,cm^{-1}$.

J	Wavenumbers/cm^{-1}					
1	45·64	2225·09	2377·45			
2	131·46	223·60	2296·49	2405·37	2465·88	
3	251·05	375·86	2393·31	2558·92	2593·68	2796·70
4	402·29	580·70	778·10	2517·79	2751·09	2767·01
	2944·04	2984·46				
5	585·41	832·07	1013·75	2671·87	2950·40	3003·91
	3181·46	3217·21	3556·47			
6	800·57	1122·02	1300·53	1648·63	2856·36	3178·69
	3271·57	3466·17	3499·66	3787·93	3791·03	
7	1047·61	1442·85	1640·54	1966·50	3071·57	3437·39
	3564·66	3782·35	3840·47	4034·95	4102·48	4145·01
8	1326·21	1790·84	2031·47	2327·51	2799·75	3317·61
	3725·94	3884·21	4128·33	4229·03	4310·40	4454·45
	4509·16	4775·65				
9	1635·99	2165·93	2466·50	2732·01	3194·69	3594·53
	4043·79	4231·39	4504·47	4617·08	4652·05	4843·46
	4921·34	5146·54	5283·55			
10	1976·52	2568·74	2937·04	3181·39	3626·44	3902·35
	4191·34	4390·44	4606·58	4907·11	4956·94	5100·23
	5268·98	5381·05	5545·93	5701·17	5802·02	
11	2347·32	2999·31	3434·54	3677·37	4094·17	4241·07
	4657·46	4765·36	5009·63	5311·13	5352·80	5569·18
	5729·33	5884·83	5973·88	6149·88	6212·83	6272·99
12	2747·92	3457·28	3953·06	4219·27	4597·18	4610·76
	5152·90	5168·09	5440·09	5712·34	5780·45	5807·36
	6058·01	6221·68	6424·91	6431·42	6571·11	6630·30
	6780·03	6852·22				
13	3177·79	3942·00	4490·94	4801·85	5011·25	5135·71
	5598·21	5677·05	5897·33	6140·28	6290·14	6312·95
	6567·15	6742·26	6914·74	6963·63	6997·27	7142·23
	7255·41	7322·84	7463·98			
14	3636·38	4452·72	5048·76	5416·63	5442·76	5710·16
	6055·12	6229·03	6380·60	6597·27	6797·60	6865·45
	7096·97	7287·07	7388·30	7427·76	7524·11	7589·48
	7683·51	7689·22	7901·44	8017·14	8197·44	
15	4123·13	4988·60	5626·94	5904·23	6055·23	6322·58
	6538·35	6807·99	6889·12	7083·90	7328·57	7438·46
	7647·36	7843·75	7853·48	7969·02	8119·61	8147·37
	8196·43	8260·90	8514·22	8591·38	8676·16	8753·39
16	4637·44	5548·71	6225·05	6396·56	6708·13	6974·50
	7047·51	7410·17	7424·76	7600·36	7881·93	8031·74
	8217·49	8332·45	8434·39	8538·20	8637·12	8723·24
	8812·47	8867·55	9147·64	9171·11	9196·02	9335·83
	9365·69	9381·60				
17	5178·70	6132·12	6841·41	6920·10	7371·06	7581·63
	7664·74	7974·92	8047·29	8146·50	8457·01	8644·73
	8806·26	8850·99	9031·47	9133·15	9157·43	9338·39
	9438·93	9501·61	9689·98	9785·69	9845·22	9894·67
	9944·34	9960·99	10038·65			
18	5746·23	6737·78	7457·07	7492·14	8043·50	8141·66
	8384·57	8552·47	8706·64	8721·76	9052·54	9277·03
	9391·36	9420·76	9641·60	9706·74	9753·54	9966·26
	10079·35	10156·29	10243·79	10417·12	10440·85	10530·07
	10550·09	10580·59	10688·41	10775·15		

Table 8 (*continued*).

	Wavenumbers/cm^{-1}					
19	6339·34	7364·71	8044·26	8138·90	8713·57	8739·88
	9122·25	9154·34	9325·20	9396·01	9667·73	9927·83
	9966·84	10046·28	10254·04	10300·84	10392·70	10606·77
	10734·13	10825·77	10827·83	11014·84	11065·06	11150·21
	11228·35	11253·45	11340·51	11369·18	11543·21	11589·29
20	6957·24	8011·79	8652·67	8808·63	9328·80	9428·63
	9770·92	9875·63	9954·54	10119·79	10301·07	10566·90
	10597·10	10691·81	10864·73	10940·45	11049·83	11260·35
	11402·01	11438·62	11507·76	11614·44	11725·79	11789·88
	11908·55	11963·04	11982·20	11998·39	12206·70	12252·54
	12328·81	12426·94				

Table 9. H_2D^+ rotational levels with j even and f ($p = 1$) total parity relative to the $J = 0$ ground state at $-32962{\cdot}24$ cm^{-1}.

J	Wavenumbers/cm^{-1}					
1	2383·71					
2	218·41	2393·45	2486·64			
3	354·33	2517·44	2638·16	2796·63		
4	530·63	777·76	2676·26	2834·14	2942·59	2984·86
5	744·08	1011·06	2867·33	3068·50	3173·44	3220·10
	3556·47					
6	991·93	1289·47	1648·62	3089·30	3334·84	3447·42
	3504·52	3788·01	3827·71			
7	1272·33	1610·42	1966·36	3341·67	3629·60	3759·42
	3837·81	4102·48	4143·55	4259·00		
8	1584·12	1970·44	2326·68	2799·75	3624·25	3952·18
	4105·06	4215·47	4455·16	4503·51	4568·39	4895·37
9	1926·56	2365·77	2728·58	3194·69	3936·88	4302·73
	4481·31	4630·56	4846·96	4902·14	4912·20	5282·40
	5342·83					
10	2299·06	2792·97	3170·49	3626·41	4191·34	4279·44
	4681·14	4886·06	5075·04	5268·76	5292·10	5345·77
	5698·25	5770·96	5802·33			
11	2701·06	3249·26	3650·10	4093·99	4651·69	4657·49
	5087·06	5317·79	5541·46	5676·58	5764·15	5820·34
	6144·60	6228·35	6271·51	6606·44		
12	3131·98	3732·61	4164·29	4596·56	5053·53	5152·92
	5520·00	5775·39	5780·47	6025·05	6110·76	6279·68
	6329·34	6622·45	6713·07	6775·47	7018·64	7118·93
13	3591·21	4241·56	4709·46	5133·13	5484·76	5677·05
	5979·48	6257·82	6312·93	6520·82	6581·69	6819·90
	6876·02	7132·49	7224·63	7311·67	7432·88	7643·67
	7701·47					
14	4078·13	4774·99	5281·85	5702·53	5945·15	6229·03
	6464·96	6764·27	6865·42	7024·72	7094·24	7376·09
	7457·30	7524·11	7676·13	7763·37	7872·05	7883·66
	8175·28	8181·28	8268·68			
15	4592·07	5331·91	5878·02	6303·09	6434·67	6808·04
	6975·96	7293·95	7438·40	7545·42	7639·60	7949·20
	8060·37	8119·64	8253·43	8331·38	8354·38	8471·47
	8670·13	8730·89	8862·27	8976·35		

Table 9 (*continued*).

	Wavenumbers/cm^{-1}					
16	5132·33	5911·32	6495·02	6930·72	6954·68	7413·25
	7511·95	7845·82	8031·55	8089·99	8209·66	8539·67
	8675·26	8723·44	8852·75	8864·25	8938·90	9088·72
	9188·27	9308·44	9381·60	9475·52	9580·80	9669·24
17	5698·22	6512·27	7130·62	7497·96	7589·57	8042·68
	8074·08	8419·50	8643·74	8660·57	8801·55	9147·36
	9299·31	9339·14	9396·38	9475·39	9589·65	9726·84
	9734·96	9911·03	10038·64	10105·89	10208·56	10221·41
	10350·44					
18	6288·98	7133·73	7783·12	8072·70	8267·35	8653·71
	8703·78	9014·55	9253·36	9277·91	9413·66	9771·90
	9930·28	9965·98	9970·26	10106·32	10273·41	10305·40
	10387·42	10540·60	10688·41	10751·73	10795·53	10862·97
	10927·94	11062·80	11100·60			
19	6903·86	7774·75	8451·18	8674·88	8963·72	9262·20
	9384·30	9630·76	9872·46	9928·34	10045·16	10412·77
	10546·07	10594·76	10612·94	10753·90	10903·24	10973·51
	11065·12	11199·47	11340·51	11391·89	11421·14	11512·16
	11550·81	11680·95	11732·78	11834·42		
20	7542·06	8434·32	9133·70	9303·98	9674·68	9892·72
	10089·44	10267·79	10513·53	10597·50	10694·93	11069·76
	11169·69	11251·87	11274·73	11418·34	11525·76	11677·78
	11757·28	11894·22	11998·17	12021·47	12098·01	12138·68
	12235·87	12321·02	12383·19	12465·13	12629·12	12704·62

Table 10. H_2D^+ rotational levels with j odd and e ($p = 0$) total parity relative to the $J = 0$ ground state at $-32962{\cdot}24\,\text{cm}^{-1}$.

J	Wavenumbers/cm^{-1}					
1	59·96	2236·98	2358·31			
2	138·67	2300·69	2452·19	2544·51		
3	253·69	457·82	2394·39	2585·28	2629·24	2691·65
4	403·08	644·77	2517·95	2751·99	2809·06	2889·44
	3135·56					
5	585·61	875·41	1175·90	2671·72	2949·98	3028·15
	3136·19	3330·50	3365·21			
6	800·59	1146·34	1452·48	2855·99	3178·54	3282·39
	3427·21	3606·08	3639·32	3791·00		
7	1047·57	1453·94	1773·59	2191·52	3070·93	3437·31
	3568·83	3756·07	3925·37	3958·06	4035·12	4310·99
8	1326·12	1795·06	2137·66	2548·67	3316·58	3725·83
	3885·67	4115·57	4287·40	4308·78	4323·17	4662·25
	4722·26					
9	1635·84	2167·31	2542·15	2945·72	3468·14	3592·96
	4043·62	4231·83	4500·18	4616·65	4688·12	4730·13
	5046·91	5120·45	5149·03			
10	1976·28	2569·12	2983·72	3381·80	3899·31	3900·08
	4390·18	4606·66	4906·48	4956·41	5119·43	5183·00
	5465·82	5547·72	5560·91	5879·26		
11	2346·96	2999·40	3458·63	3855·85	4237·75	4363·84
	4764·99	4963·92	5009·59	5310·74	5352·91	5577·67
	5674·10	5919·44	5980·99	6034·50	6201·25	6399·26

Table 10 (*continued*).

	Wavenumbers/cm^{-1}					
12	2747·36	3457·29	3963·24	4366·47	4606·07	4860·72
	5167·54	5439·97	5463·75	5711·47	5807·69	6061·01
	6194·16	6403·97	6450·12	6542·44	6556·56	6846·87
	6875·08					
13	3176·98	3942·00	4494·40	4911·62	5005·25	5389·11
	5597·53	5897·26	5988·50	6138·98	6290·43	6567·93
	6635·58	6734·11	6905·21	6945·76	6972·82	7081·49
	7249·26	7377·90	7476·28			
14	3635·22	4452·72	5049·62	5434·35	5488·90	5948·16
	6054·17	6380·39	6537·95	6595·41	6797·77	7096·99
	7199·88	7287·94	7366·52	7424·14	7546·68	7647·79
	7679·56	7908·98	8031·38	8124·09		
15	4121·53	4988·59	5627·02	5894·20	6094·27	6533·64
	6540·55	6888·53	7081·40	7111·53	7328·70	7647·23
	7778·62	7818·85	7855·32	7968·17	8138·39	8156·68
	8241·00	8441·02	8469·52	8607·79	8667·05	8711·57
16	4635·28	5548·69	6224·96	6384·25	6724·40	7045·34
	7155·42	7420·39	7597·19	7708·41	7882·19	8217·33
	8302·88	8373·35	8436·18	8538·55	8626·68	8787·68
	8861·19	9059·70	9067·90	9155·02	9210·06	9323·17
	9365·69					
17	5175·86	6132·05	6840·80	6905·81	7375·41	7579·50
	7801·25	7975·00	8142·80	8327·91	8457·43	8802·40
	8821·08	8984·26	9032·15	9132·57	9146·86	9427·58
	9507·61	9671·93	9688·68	9696·51	9828·40	9888·50
	9950·41	9971·34	10187·50			
18	5742·59	6737·65	7443·71	7488·02	8043·48	8138·90
	8472·77	8552·04	8717·70	8969·11	9053·61	9355·97
	9418·26	9610·52	9640·56	9696·05	9753·83	10074·85
	10169·24	10226·54	10327·68	10348·70	10438·50	10468·10
	10537·74	10625·72	10773·48	10803·92		
19	6334·76	7364·43	8024·76	8138·26	8711·04	8738·14
	9143·50	9175·45	9320·77	9629·94	9671·41	9926·18
	10044·98	10241·11	10255·07	10298·79	10392·69	10732·50
	10807·10	10837·80	10971·71	11011·10	11035·84	11125·25
	11158·35	11303·02	11365·94	11441·80	11584·51	11688·42
20	6951·61	8011·27	8630·18	8808·35	9324·47	9428·29
	9766·61	9888·78	9950·05	10291·41	10328·33	10522·88
	10690·35	10848·33	10909·84	10944·91	11049·56	11399·61
	11419·47	11512·24	11609·74	11625·58	11723·10	11780·62
	11848·46	11976·66	11996·96	12103·59	12202·07	12365·39
	12373·48					

Table 11. H_2D^+ rotational levels with j odd and $f(p = 1)$ total parity relative to the $J = 0$ ground state at $-32962{\cdot}24\,\text{cm}^{-1}$.

J	Wavenumbers/cm^{-1}					
1	72·37	2256·86				
2	175·71	2357·94	2543·57			
3	325·72	459·30	2498·78	2634·23	2685·24	
4	515·44	653·68	2668·90	2831·92	2869·64	3135·63

Table 11 (*continued*).

	Wavenumbers/cm^{-1}					
5	737·74	902·86	1175·97	2864·89	3076·21	3101·30
	3330·73	3365·66				
6	989·74	1204·37	1453·14	3088·58	3340·35	3394·36
	3607·12	3641·49	3979·94			
7	1271·66	1551·43	1776·93	2191·53	3341·50	3631·49
	3728·32	3925·85	3967·29	4258·47	4311·04	
8	1583·94	1935·61	2149·28	2548·70	3624·27	3952·53
	4089·79	4281·86	4347·13	4567·56	4662·58	4723·15
9	1926·53	2348·73	2571·97	2945·90	3468·14	3937·00
	4302·66	4474·81	4672·54	4776·97	4907·25	5047·77
	5123·07	5335·45				
10	2299·06	2786·05	3043·36	3382·63	3899·36	4279·63
	4681·04	4883·62	5095·77	5247·73	5277·53	5467·34
	5565·18	5766·63	5959·93			
11	2701·08	3246·90	3557·18	3858·95	4363·84	4652·00
	4963·92	5087·02	5317·02	5548·27	5678·52	
	5921·61	6049·07	6222·60	6408·95	6538·87	6554·01
12	3132·01	3731·95	4104·92	4375·85	4860·74	5053·93
	5463·73	5520·00	5775·21	6025·49	6111·68	6275·69
	6410·19	6574·46	6704·02	6885·63	7020·14	7037·03
13	3591·27	4241·44	4677·67	4935·12	5389·22	5485·42
	5979·41	5988·63	6257·91	6520·05	6581·71	6635·58
	6818·79	6932·19	7139·07	7211·17	7391·03	7435·61
	7565·75	7667·28				
14	4078·21	4774·99	5268·24	5537·21	5943·60	5951·09
	6464·97	6537·99	6764·41	7024·49	7093·62	7199·89
	7377·02	7485·41	7730·90	7750·73	7881·13	7925·05
	8125·34	8180·26	8249·58			
15	4592·18	5331·92	5873·67	6178·31	6435·25	6539·39
	6975·89	7111·55	7294·14	7545·47	7639·12	7778·67
	7950·89	8066·46	8295·67	8354·78	8373·09	8441·03
	8487·75	8671·26	8715·70	8847·06	9042·07	
16	5132·48	5911·34	6494·26	6850·43	6953·73	7161·28
	7511·67	7708·44	7846·27	8090·04	8209·43	8373·55
	8541·22	8670·71	8861·32	8879·48	9018·67	9067·07
	9078·35	9189·58	9336·99	9459·46	9620·14	9670·21
17	5698·41	6512·28	7130·80	7499·01	7545·77	7816·93
	8071·97	8327·96	8420·37	8659·91	8801·28	8984·89
	9148·54	9293·93	9400·98	9481·22	9679·25	9692·93
	9699·20	9735·50	9988·67	10086·09	10219·79	10224·87
	10341·30	10349·10				
18	6289·23	7133·76	7783·34	8074·46	8250·68	8509·18
	8656·29	8968·92	9016·71	9254·74	9413·20	9612·31
	9772·76	9929·56	9972·16	10106·75	10306·71	10325·20
	10337·15	10359·79	10665·20	10728·95	10795·90	10855·06
	10925·08	11029·09				
19	6904·18	7774·81	8451·32	8676·97	8961·34	9235·99
	9266·34	9622·14	9644·40	9873·50	10044·28	10255·66
	10413·73	10551·61	10600·00	10752·82	10904·81	10970·14
	11000·42	11042·49	11345·25	11396·92	11405·85	11511·05
	11524·85	11682·22	11699·75	11765·62	11835·06	
20	7542·47	8434·41	9133·87	9306·37	9676·74	9892·81
	9999·52	10265·73	10326·32	10514·91	10693·44	10915·17
	11071·38	11176·56	11266·17	11417·49	11527·53	11624·20
	11684·29	11736·45	12017·43	12027·13	12110·53	12152·55

Table 12. Symmetry labels and sizes of the rotational manifolds (M_v) for H_2D^+.

Point group [7]	Parity of j†	Total parity‡	$v = 0$§		M_v‖		
			K_a	K_c	$v = 0$	$v_2 = 1$	$v_3 = 1$
A_1	e	e	$2n-2$	$J+2-2n$	$J/2+1$	$J/2+1$	$(J+1)/2$
A_2	o	e	$2n-1$	$J+2-2n$	$(J+1)/2$	$(J+1)/2$	$J/2+1$
B_1	e	f	$2n$	$J+1-2n$	$J/2$	$J/2$	$(J+1)/2$
B_2	o	f	$2n-1$	$J+1-2n$	$(J+1)/2$	$(J+1)/2$	$J/2$

† e = even, o = odd.
‡ e is $p = 0$, f is $p = 1$. Total parity is $(-1)^{J+p}$.
§ $n = 1, 2, \ldots, M_{v=0}$.
‖ Manifold size using integer arithmetic.

5. Discussion

From the results shown in table 7 it is possible to make an assessment of the likely error in our calculations arising from the chosen potential. In fact the agreement between the results obtained from the SDL and BVDH potentials is fairly good, the largest difference being about $30\,cm^{-1}$ for a few of the higher states. A detailed comparison of the levels shows a number of systematic features which it is possible to understand from a knowledge of the results obtained at low J with each of the potentials.

The frequencies of the lowest 3 states with j even or odd and a number of the higher ones (for example, both states 16) are found to be 2–6 cm^{-1} higher for the SDL than the BVDH potential. Examination of the wavefunction shows that such states can, at least approximately, be associated with the vibrational ground state. The previous calculations [3] for low J showed that a precisely similar discrepancy was observed in the ground vibrational state results. The discrepancy may be thought of as due to the discrepancy between the calculated rotational constants in each potential and because the terms in the energy proportional to these constants are multiplied by J^2, the difference will be magnified when dealing with high J states.

On the other hand for certain states (for example both states number 11) the SDL potential gives frequencies that are 10–20 cm^{-1} *lower* than the BVDH potential. Examination of the wavefunctions show that such states are in fact associated, approximately, with the v_2 and v_3 vibrationally excited states. This discrepancy is again to be expected from previous calculations where it was shown that the SDL potential gives v_2 and v_3 fundamental frequencies which are about $20\,cm^{-1}$ too low. That the discrepancy is generally less than this is due to a cancellation of errors. There are a few levels, both states number 17 for example, for which the SDL frequencies are up to $30\,cm^{-1}$ lower than the BVDH ones. These levels can be associated with states with 2 quanta in the v_2 and v_3 modes, probably $2v_2$, for which discrepancies of this magnitude between the potentials are to be expected [3].

Not all the states fall exactly into the three categories given above, which can be explained by the mixed vibrational parentage of some states and the simplistic treatment of the rotational constants in the above discussion. However, it is clear that the comparative behaviour of the two potentials can be understood from their properties at low J. It is worth noting that, although the absolute shifts for $J = 16$

levels are as much as $30\,cm^{-1}$, transitions in simulated spectra, which of course only involve $\Delta J = 0, \pm 1$, will generally agree to about $1\,cm^{-1}$ provided the transitions involve no vibrational excitation.

Figures 1 and 2 illustrate the qualitative behaviour of the results of tables 8 to 11. Figure 1 shows the broadening of the rotational manifolds for one symmetry block (the total symmetric *ee* block) as J increases. For comparison, the position of the lowest 10 band origins are given for $J = 0$. What figure 1 shows is the progressive overlap of the rotational manifolds belonging to different vibrational states. Thus for $J = 4$ and above, the ν_2 and ν_3 states become significantly mixed, something that is known from both theory [2] and experiment [10, 12]. Above $J = 11$ the rotational levels of the ground state overlap those of the vibrationally excited states. By $J = 20$ the lowest ν_2 level is the third excited state. It is thus possible to extrapolate to $J \sim 25$ where one will find that the lowest vibrational excitation is less than the lowest rotational excitation!

In most of the previous work on highly-excited rotational states the molecule has been treated as a rigid asymmetric top. It is well-known [7, 25] that this model predicts a large number of accidental degeneracies, with splittings as small as $10^{-13}\,cm^{-1}$ when $\kappa = 0$ and $J = 20$ [7]. It is interesting to see how far this structure is preserved when the constraints of rigidity and no ro-vibrational interaction are lifted. Figure 2 gives the levels of $J = 15$ plotted to emphasize the

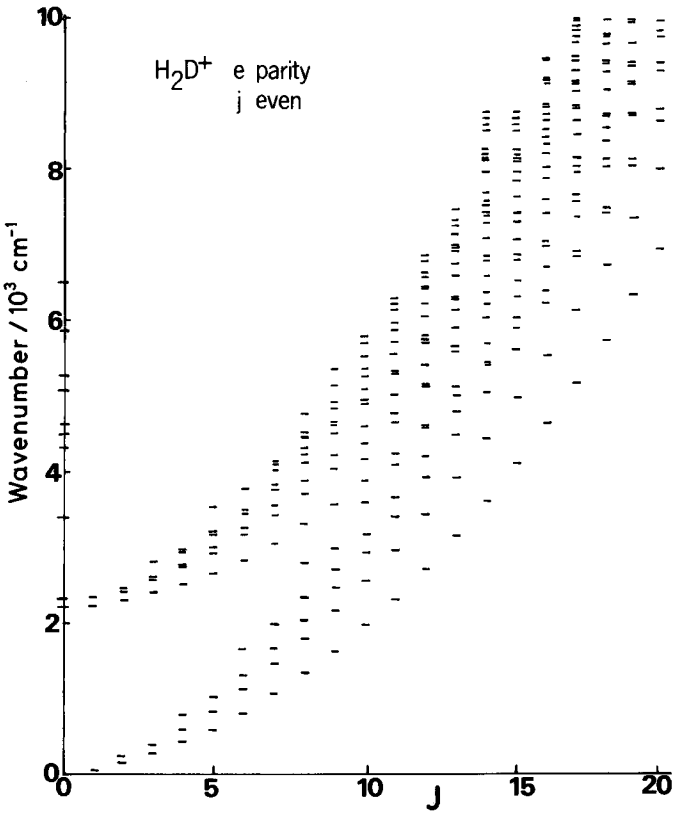

Figure 1. Rotational levels associated with the lowest three vibrational states of H_2D^+ as a function of J. Results are for the symmetry block with j even (para H_2) and e ($p = 0$) total parity.

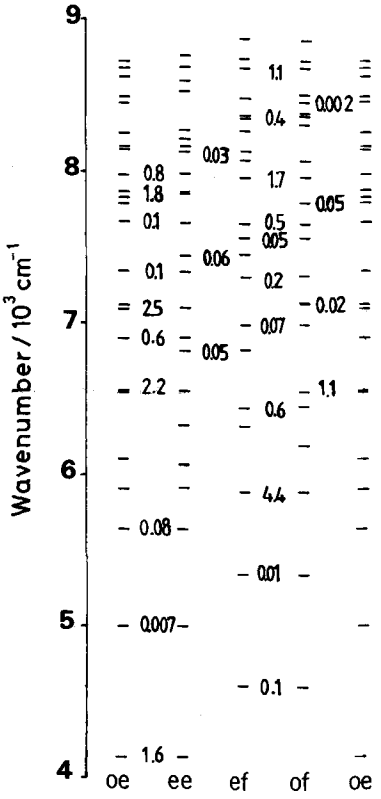

Figure 2. Comparison between symmetry species for rotational levels with $J = 15$. The figures give the splittings, in cm^{-1}, of near degenerate levels between neighbouring symmetries. The symmetries are labelled by parity of j (e for even, o for odd) and total parity (e for $p = 0$ and f for $p = 1$), see table 12.

degeneracies. The separation of all levels closer than $5\,cm^{-1}$ are given explicitly. Splittings of less than $0{\cdot}01\,cm^{-1}$ can have no significance because of the convergence criteria of the diagonalization and it should be remembered that the absolute convergence of the $J = 15$ calculation is only about $1\,cm^{-1}$, although the splittings between systematically degenerate levels are probably better converged.

Inspection of figure 2 shows that the structure of the nearly degenerate levels corresponds, for the lowest levels, with that found by Harter and Patterson for a rigid asymmetric top with $\kappa = 0$ [7]. The lowest states are three nearly degenerate pairs for each total parity: each pair is composed of one state with j even and one with j odd, the so-called $C_2(x)$-Type Clusters [7].

At higher energy there are another 3 interleaved pairs, this time with the members of each pair having a common j parity and differing in the total parity, the so-called $C_2(z)$-Type Clusters [7]. Overlapping the higher degeneracies are a large number of near degeneracies with common j parity and differing in total parity. These come from rotational states associated with vibrationally excited states. However, because of the overlap between the levels associated with vibrational states ν_2 and ν_3, and no doubt higher vibrational states, there is no easily discernible structure in this energy region. One would expect that for $J \gg 15$ the structure of the rotational manifold of the vibrational ground state would also be destroyed.

6. Conclusion

In this paper we propose a method of performing calculations on the highly rotationally excited state of triatomic molecules. The method is in principle exact within the constraints of the variation theorem, which we apply twice. We use the method to calculate the rotational levels with $J \leqslant 20$ of the lowest three vibrational state of H_2D^+, a molecule chosen because of the likely strength of Coriolis and centrifugal distortion effects. Qualitatively, we see the progressive overlap of rotational manifolds belonging to different vibrational states. We thus probe both low and intermediate J regions and expect the high J region, where the width of a rotational manifold is much greater than the vibrational spacing, to be reached at $J \sim 25$ for H_2D^+.

We hope that our results might aid the observation of high J states of H_2D^+. There are two main sources of error in our calculations caused by inaccuracies in the underlying electronic potential and truncation of the vibrational basis sets. By comparing results for different potentials we see that the absolute energy of the lowest states vary by about $5\,cm^{-1}$ for $J = 16$, where the variational calculations are converged to about $1\,cm^{-1}$. Transition frequencies, which do not involve vibrational excitation, will allow for a cancellation of much of this absolute error and should be accurate to about $1\,cm^{-1}$ for $J \sim 15$ and $5\,cm^{-1}$ for $J \sim 20$, where the convergence of the basis set is poorer.

We are grateful to Professor J.-L. Destombes for bringing this problem to our attention and for helpful correspondence.

References

[1] Tennyson, J., and Sutcliffe, B. T., 1984, *Molec. Phys.*, **51,** 887.
[2] Tennyson, J., and Sutcliffe, B. T., 1985, *Molec. Phys.*, **54,** 141.
[3] Tennyson, J., and Sutcliffe, B. T., 1985, *Molec. Phys.*, **56,** 1175.
[4] Tennyson, J., and Sutcliffe, B. T., 1986, *J. chem. Soc. Faraday* II (in the press)
[5] Spirko, V., Jensen, P., Bunker, P. R., and Cejchan, A., 1985, *J. molec. Spectrosc.*, **112,** 183. Jenson, P., Spirko, V., and Bunker, P. R., 1986, *J. molec. Spectrosc.*, **115,** 269.
[6] Lemoine, B., Bogéy, M., and Destombes, J. L., 1985, *Chem. Phys. Lett.*, **117,** 532.
[7] Harter, W. G., and Patterson, C. W., 1984, *J. chem. Phys.*, **80,** 4241.
[8] Bohr, A., and Mottelson, B. R., 1975, *Nuclear Structure*, Vol. II (Benjamin), Chap. 4.
[9] Chen, C.-L., Maessen, B., and Wolfsberg, M., 1985, *J. chem. Phys.*, **83,** 175.
[10] Shy, J.-T., Farley, J. W., and Wing, W. H., 1981, *Phys. Rev.* A, **24,** 1146.
[11] Amano, T., and Watson, J. K. G., 1984, *J. chem. Phys.*, **81,** 2869.
[12] Foster, S. C., McKellar, A. R. W., Peterkin, I. R., Watson, J. K. G., Pan, F. S., Crofton, M. W., Altman, R. S., and Oka, T., 1986, *J. chem. Phys.*, **84,** 91.
[13] Bogey, M., Demuynck, C., Denis, M., Destombes, J. L., and Lemoine, B., 1984, *Astron. Astrophys.*, **137,** L15. Warner, H. E., Conner, W. T., Petrmichl, R. H., and Woods, R. C., 1984, *J. chem. Phys.*, **81,** 2514. Saito, S., Kawaguchi, K., and Hirota, E., 1985, *J. chem. Phys.*, **82,** 45.
[14] Destombes, J. L. (private communication).
[15] Sutcliffe, B. T., and Tennyson, J., 1986, *Molec. Phys.*, **58,** 1053.
[16] Tennyson, J., 1986, *Comput. Phys. Rep.* (in the press).
[17] Subroutine EIGSFM, Garbow, B. S., Boyle, J. M., Dongarra, J. J., and Moler, C. B., 1977, *Matrix Eigensystem Routines—EISPACK Guide Extension* (Lecture Notes in Computer Science, Vol. 51) (Springer).
[18] Subroutines BANDR and BISECT [17].

[19] FO2FJF, 1983, NAG Fortran Library Manual, Mark 11, Vol. 4. NIKOLAI, P. J., 1979, *ACM Trans. Math. Software*, **5,** 118.
[20] TENNYSON, J., 1983, *Comput. phys. Commun.*, **29,** 307.
[21] SCHINKE, R., DUPUIS, M., and LESTER, W. A., JR., 1980, *J. chem. Phys.*, **72,** 3909.
[22] WATSON, J. K. G., FOSTER, S. C., MCKELLAR, A. R. W., BERNATH, P., AMANO, T., PAN, F. S., CROFTON, M. W., ALTMAN, R. S., and OKA, T., 1984, *Can. J. Phys.*, **62,** 1875.
[23] MARTIRE, B., and BURTON, P. G., 1985, *Chem. Phys. Lett.*, **121,** 479.
[24] BURTON, P. G., VON NAGY-FELSOBUKI, E., DOHERTY, G., and HAMILTON, M., 1985, *Molec. Phys.*, **55,** 527.
[25] GORDY, W., and COOK, R. L., 1970, *Microwave Molecular Spectra*, 2nd edition, (Interscience-Wiley), Appendix 1. TOWNES, C. H., and SCHAWLOW, A. L., 1955, *Microwave Spectroscopy* (McGraw-Hill), Appendix IV.